

XIAOCHANG LI (ORCID: 0009-0005-3891-4566)¹

XIANJUN LYU (ORCID: 0000-0001-6818-6110)¹

STUDY ON THE TREATMENT OF FLUORINE-CONTAINING WASTEWATER BY PRECIPITATION-ADSORPTION PROCESS

Fluorine-containing wastewater from the Yuncheng Sewage Treatment Plant in Heze City, Shandong Province was treated by coagulation and precipitation with poly aluminum sulfate, and CaO chemical precipitation-activated carbon adsorption, with a view to reducing fluoride ions concentration in the wastewater to below the discharge standard. The results showed that the optimum conditions for the coagulation-sedimentation test of poly aluminum sulfate were as follows: the dosage of poly aluminum sulfate 0.3 g/dm³, initial pH value 4.0, the removal rate of fluoride ion in the fluorine-containing wastewater reached 98.46%, and the concentration of fluoride ion was 0.462 mg/dm³, which reached the discharge standard (1.5 mg/dm³); The optimum conditions for the CaO chemical precipitation, and lanthanum loaded activated carbon adsorption method were as follows: the amount of CaO 20 g/dm³, initial pH of the chemical precipitation test 8.0, the dosage of lanthanum loaded activated carbon 10 g/dm³, and the initial pH of the adsorption test 6.0. At this time, the removal rate of fluoride ions in the fluorine-containing wastewater reached 95.81%, and the concentration of fluoride ions was 1.26 mg/dm³, which also met the discharge standard.

1. INTRODUCTION

The fluorine content in groundwater is generally 1.0~3.0 mg/dm³, and it can reach 10–20 mg/dm³ in high-fluorine areas [1, 2]. Residents living in high-fluorine areas will suffer from tooth, and bone fluorosis if drinking water contains excessive fluoride for a long time [3]. Fluorine pollution can also poison animals, and plants, thus affecting agricultural, and animal husbandry production. In industry, wastewater discharged from fluorine-containing ore mining, metal smelting, aluminum processing, electronics, electroplating, pesticides, and other industries often contains high concentrations of fluo-

¹ College of Chemical and Biological Engineering, Shandong University of Science and Technology, Qingdao 266590, Shandong, China, corresponding author X. Lyu, email address: lyuxianjun@163.com

ride, causing environmental pollution [4–6]. According to the provisions of the *Environmental Quality Standard for Surface Water (GB 3838-2002)*, the content of fluoride ions in waters of the I, II, and III class shall not be higher than 1.0 mg/dm³, in waters of the IV, and V class not than 1.5 mg/dm³.

Aluminum salt has a good removal effect on fluoride ions [7–9], so poly aluminum sulfate was selected as the coagulant, and precipitator in this work. The influence of the dosage of reagent, and initial pH on the removal rate of fluoride ions in fluorine-containing wastewater was investigated, and the influence mechanism of these factors was briefly described. The CaO chemical precipitation method is commonly used to treat fluoride ions [10–12] but the treatment effect is limited due to CaO solubility, and the wastewater cannot be treated below the discharge standard when used alone [13, 14]. Thus the adsorption method is added to treat the wastewater up to the standard. Due to its large specific surface area, activated carbon is a commonly used adsorbent in water treatment [15, 16], while rare earth elements have strong selective adsorption for fluoride ions [17–19]. Thus, in this work, lanthanum modified activated carbon was used as an adsorbent. Fluorine-containing wastewater from Yuncheng Sewage Treatment Plant was treated by the poly aluminum sulfate coagulation-sedimentation and CaO precipitation-activated carbon adsorption methods.

2. MATERIALS AND METHODS

Fluorine-containing wastewater. Wastewater used in this test was taken from Yuncheng Sewage Treatment Plant, Heze City, Shandong Province, China. According to the national standards, some wastewater quality indicators were determined, and the results are shown in Table 1.

Table 1

Parameters of wastewater from Yuncheng Sewage Treatment Plan

Fluoride ions concentration [mg/dm ³]	COD [mg/dm ³]	pH
30.05	100	7.8

Chemicals. Poly aluminum sulfate selected in this test is a white solid powder from the Zhengzhou Gongyi Tenglong Water Treatment Materials Co., Ltd. Its main components are given in Table 2.

Table 2

Main components of poly aluminum sulfate [%]

Al ₂ O ₃	Water insoluble substance	Arsenic (As)	Heavy metals
15.6	0.14	0.0004	0.002

CaO (analytical reagent) originated from Tianjin Beilian Fine Chemicals Development Co., Ltd. Its phase composition was analyzed by X-ray diffraction (XRD, Rigaku Utima IV) (Fig. 1). The purity of CaO used was high, water was adsorbed during the measurement process, thus $\text{Ca}(\text{OH})_2$ was identified in the XRD pattern.

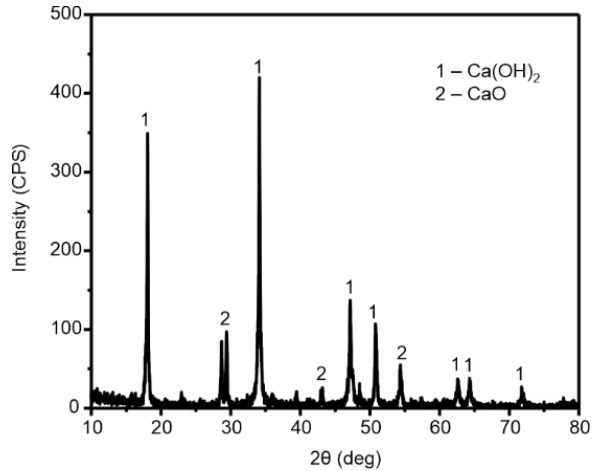


Fig. 1. XRD spectrum of CaO (CPS – counts/s)

Activated carbon from Charnaugh High-end Activated Carbon Company, included coconut shell (YK), and coal-based (MJ) carbon. Its characteristics is given in Table 3.

Table 3

Results of performance tests of activated carbon

Activated carbon type	MJ	YK
Methylene blue adsorption value, mg/g	111	97.5
Specific surface area, m^2/g	987.36	1047.69
Grain size range (mesh)	8–30	

Coagulation and sedimentation tests with poly aluminum sulfate. At 25 °C, the effects of the dosage of poly aluminum sulfate, and initial pH on the removal rate of fluoride ions from fluoride-containing wastewater from Yuncheng Sewage Treatment Plant were studied. The dosages of poly aluminum sulfate were 0.1, 0.2, 0.3, 0.4, and 0.5 g/dm^3 . pH of the solution was adjusted by adding an appropriate volume of 1% H_2SO_4 or NaOH and measured with a pH meter (PHSJ-3F). The selected initial pH values were 2, 4, 6, 8, and 10. Initial concentration of fluoride was 30.05 mg/dm^3 . The poly aluminum sulfate before, and after the reaction was characterized by X-ray photoelectron spectroscopy (XPS, ESCALAB XI+) to study its purification mechanism. The beakers with prepared fluoride wastewater were placed on a magnetic stirrer and stirred for 15 min at

a speed of 300 rpm. The fluoride concentration of the supernatant was measured by the fluoride selective electrode method. Its removal rate was calculated using the following equation:

$$\text{Removal rate} = \frac{C_0 - C_e}{C_0} \times 100\% \quad (1)$$

where C_0 is the initial fluoride concentration, C_e fluoride concentration in the supernatant after the coagulation-sedimentation process.

CaO chemical precipitation test. At 25 °C, The dosages of CaO were 5, 10, 15, 20, and 25 g/dm³. The initial pH values were 4, 6, 8, 10, and 12. The selected initial concentration of fluoride is 30.05 mg/dm³. CaO before, and after the reaction was characterized by XPS. The beakers containing CaO at various concentrations were placed on a magnetic stirrer and stirred for 30 min at a speed of 500 rpm. the fluoride concentration of the supernatant was measured, and its removal rate was calculated (Eq. (1)).

Activated carbon adsorption batch test. The activated carbon was pretreated by washing with deionized water at a liquid:solid ratio of 3:1. Then, the activated carbon was filtered, and roasted for 10 h at 100 °C. 15 g of the pretreated activated carbon was added to 150 cm³ of lanthanum nitrate solution (0.05 mol/dm³). The mixture was shaken for 24 h at 25 °C, and after sedimentation and filtration, the activated carbon was washed with deionized water, and dried for 10 h at 70 °C. The lanthanum-modified coconut shell activated carbon (La-YK), and lanthanum-modified coal-based activated carbon (La-MJ) were obtained.

At 25 °C, the effects of the addition of La-YK and La-MJ on the removal rate of fluoride ions in fluorine-containing wastewater were studied. The initial fluoride concentration was 30.05 mg/dm³. The dosages of activated carbon were 4, 6, 8, 10, and 12 g/dm³. The initial pH was adjusted to 2, 4, 6, 8, and 10. Different quantities of activated carbon were put into a 100 cm³ wastewater sample, and different pH values were adjusted. The beakers were placed on a magnetic stirrer and stirred at a speed of 500 rpm. The fluoride ions concentration was measured after 1, 2, 5, 7, 10, 15, 20, 30, 40, and 60 min of adsorption. The activated carbon before, and after the reaction was characterized by X-ray photoelectron spectroscopy (XPS, ESCALAB XI+), and Fourier transform infrared spectroscopy (FT-IR, Nicolet iS50 FT-IR). An automatic specific surface area and porosity analyzer (BET, Mike ASAP2460) was used to study its purification mechanism for fluorine-containing wastewater. Scanning electron microscopy (SEM, Nova Nano SEM 450) was used to observe the activated carbon before, and after modification, and adsorption.

Chemical precipitation-adsorption test. The integrated process (chemical precipitation with CaO-batch adsorption) was used to treat fluorine-containing wastewater. The initial fluoride concentration was 30.05 mg/dm^3 . Firstly, 100 cm^3 of fluorine-containing wastewater was put into a beaker, and pH was adjusted to 8.0. Then, 2 g of CaO was added. The beaker was placed on a magnetic stirrer and reacted at 500 rpm for 30 min. After the reaction, the primary effluent was obtained by filtration through filter paper (qualitative filter paper, diameter 15 cm, medium speed), which was further subjected to the adsorption process with the use of La-YK or La-MJ. The adsorbent dosage was 10.0 g/dm^3 , and the initial pH 6.0. The primary effluent was placed on a magnetic stirrer and reacted at 500 rpm for 50 min. Each precipitation-adsorption experiment was repeated three times, and the average fluoride concentration after treatment was involved in the calculation of the fluoride removal rate (Eq. (1)).

3. RESULTS, AND DISCUSSION

3.1. COAGULATION AND SEDIMENTATION PERFORMANCE OF POLY ALUMINUM SULFATE

The relationship between fluoride ion removal rate, and poly aluminum sulfate dosage is given in Fig. 2. When the dosage of poly aluminum sulfate is less than 0.3 g/dm^3 , the removal rate decreases rapidly with the decrease in dosage. When the dosage is higher than 0.4 g/dm^3 , the removal rate tends to be stable with the increase in dosage. This may be due to the increase of the amount of Al^{3+} ions in water with the increase of the dosage of poly aluminum sulfate, and more F^- ions can be removed by electrostatic adsorption. The amount of fluoride ion is fixed, so when the coagulant dosage continues to increase, the F^- ions removal rate will no longer be affected by the coagulant dosage of 0.5 g/dm^3 . Considering the cost of materials, the amount of poly aluminum sulfate used in the initial pH condition test in the later stage is 0.3 g/dm^3 .

The effect of pH on the efficiency of fluoride ion removal is shown in Fig. 3. The overall trend is that the removal rate of fluoride ions decreases with the increase in pH. At pH 4.0, the removal rate reached the highest value (98.46%). When pH increased from 6 to 10, the removal rate decreased significantly. When pH is low, a high concentration of H^+ ions may promote the complexation reaction of Al^{3+} and F^- to move in a positive direction, that is, it is conducive to the removal of F^- ions. On the contrary, when pH is high, the content of negatively charged OH^- ions in water is high. There will be a certain competitive relationship between OH^- and F^- ions in the electrostatic adsorption process, so it is not conducive to the removal of F^- ions. It can be seen from this that the original pH of wastewater from the Yuncheng Sewage Treatment Plant is relatively high, and its pH should be appropriately reduced in order to reach the discharge standard stably. Under the optimal conditions, the concentration of fluoride ions

in the effluent of coagulation, and sedimentation is 0.462 mg/dm^3 , which meets the discharge requirements.

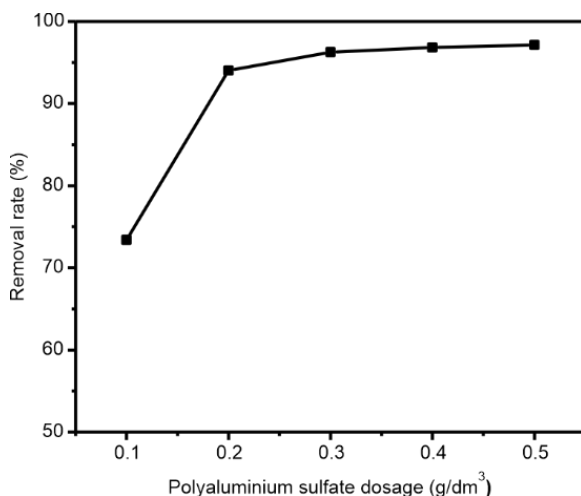


Fig. 2. Effect of poly aluminum sulfate dosage on fluoride removal rate (pH 4.0, initial F^- concentration 30.05 mg/dm^3)

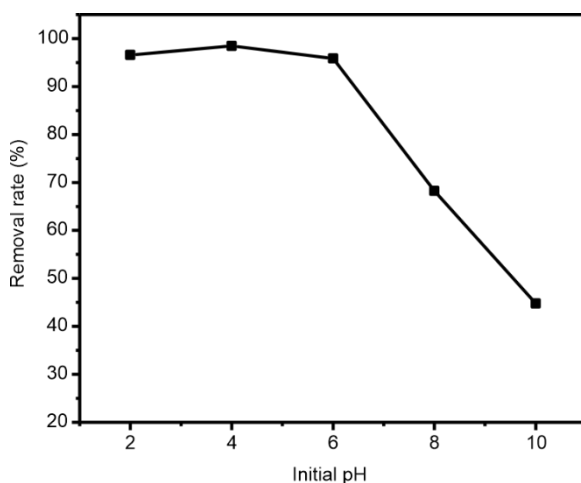


Fig. 3. Effect of initial pH on fluoride removal rate (poly aluminum sulfate dosage 0.3 g/dm^3 , initial F^- concentration 30.05 mg/dm^3)

X-ray photoelectron spectra are shown in Figs. 4 and 5. The binding energy of $\text{Al}2s$ decreased from 120.15 eV before the reaction to 118.95 eV after the reaction, and the binding energy of $\text{Al}2p$ decreased from 75.35 eV before the reaction to 74.25 eV after the reaction, and the peak areas also changed.

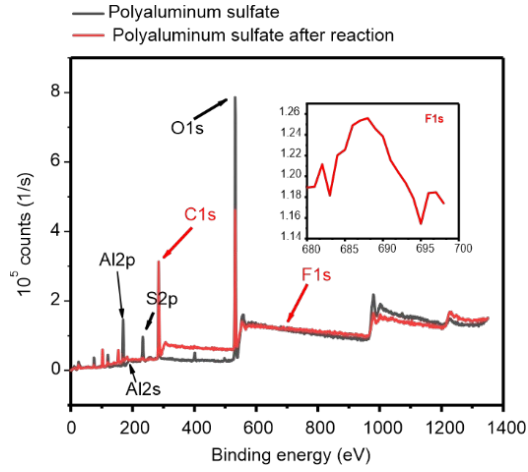


Fig. 4. XPS spectra of poly aluminum sulfate before and after reaction

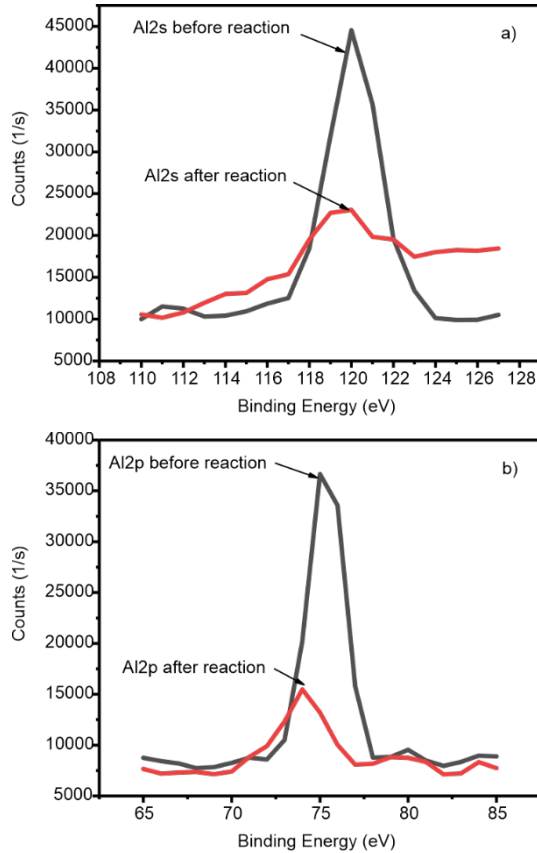


Fig. 5. XPS of Al2s (a), and Al2p (b) before and after reaction

These effects show that the fluoride removal with poly aluminum sulfate is not only the function of electrostatic adsorption but also a chemical reaction. According to the changes in the atlas, it can be deduced that Al^{3+} content is reduced during the reaction. Fluorine and carbon were detected in the XPS spectrum after the reaction, indicating that fluoride ions were removed from the wastewater, and reacted with poly aluminum sulfate into the solid phase, and poly aluminum sulfate also had a certain removal effect on the organic matter in the wastewater.

3.2. CHEMICAL PRECIPITATION PROPERTIES OF CaO

The relationship between fluoride removal rate and CaO dosage is shown in Fig. 6. The removal rate increases rapidly with the increase of the dosage from 5 to 15 g/dm^3 . When the dosage exceeds 20 g/dm^3 , the removal rate increases slowly. When the amount of CaO is 20 g/dm^3 , the concentration of fluoride ions in the supernatant is 7.79 mg/dm^3 , and the removal rate of fluoride ions is 74.08%. At this time, the amount of CaO is several times excessive. It can be seen that only when a large amount of CaO is excessive, a good effect of fluoride removal can be achieved.

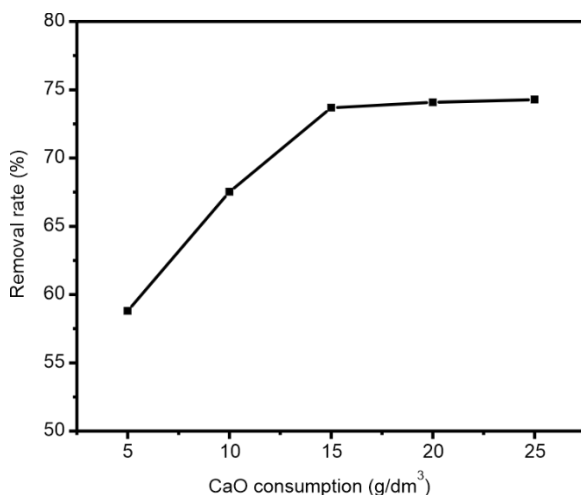


Fig. 6. Effect of CaO dosage on fluoride ion removal rate (pH 7.8, initial F^- concentration 30.05 mg/dm^3)

For the dosage of CaO equal to 20 g/dm^3 , the pH was adjusted to 4, 6, 8, 10, and 12, and the effect of pH variation on F^- removal rate is shown in Fig. 7. It can be seen that the removal rate of fluoride ions first increases, and then decreases with the increase of pH. The optimal pH is 8.0, and the optimal removal rate reaches 74.18%. This may be due to the partial consumption of CaO in a slightly acidic solution thus reducing the absolute amount of CaO, and making the removal rate low. At high pH, OH^- ions compete

with F^- ions, which is detrimental to the removal of F^- ions. The concentration of F^- ions after purification is 7.76 mg/dm^3 , higher than the emission standard (1.5 mg/dm^3). Therefore, adding the lanthanum-modified activated carbon adsorption method is considered to meet the emission standard.

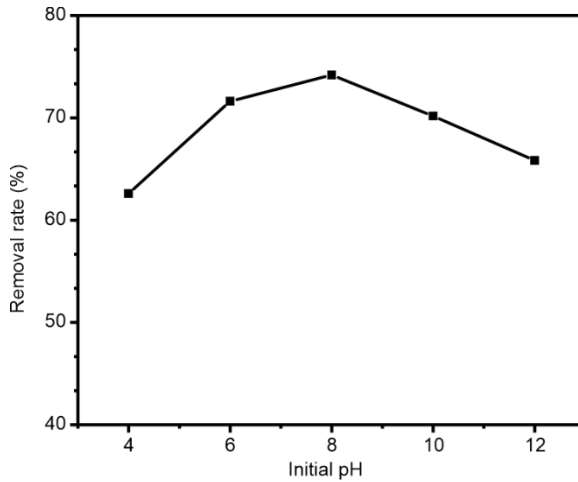


Fig. 7. Effect of initial pH on fluoride removal rate (CaO dosage 20 g/dm^3 , initial F^- concentration 30.05 mg/dm^3)

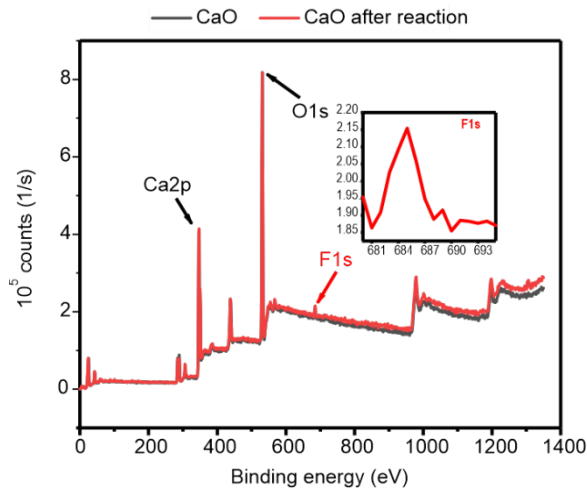


Fig. 8. XPS spectra of CaO before and after reaction

3.3. ADSORPTION PROPERTIES OF La-MODIFIED ACTIVATED CARBON

The effect of the dosage of La-YK, and La-MJ activated carbon on the removal efficiency of fluoride ions was studied is shown in Fig. 9.

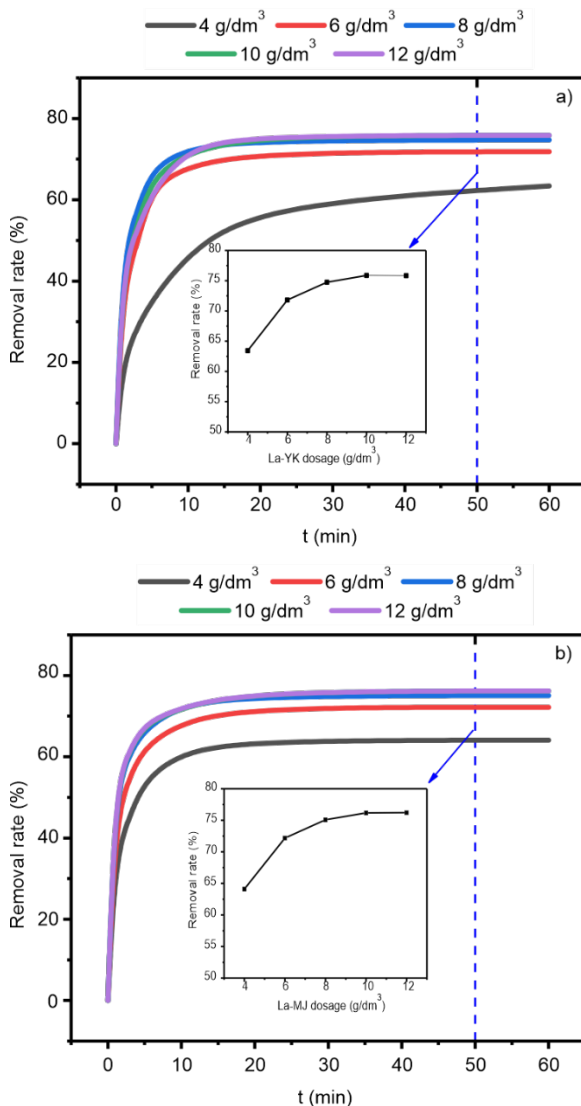


Fig. 9. Effect of La-YK (a), and La-MJ (b) dosage on fluoride ion removal rate (pH 6.0, initial F⁻ concentration 30.05 mg/dm³)

When the amount of adsorbent increases from 4.0 g/dm³ to 10.0 g/dm³, the removal rate increases rapidly, indicating that the adsorption of fluorine ions is closely related to the increase of number of adsorption sites. However, when the dosage of adsorbent increased from 10.0 g/dm³ to 12.0 g/dm³, the removal rate decreased, indicating that the activated carbon has become saturated at this dosage, and a further increase in the dos-

age will not increase the removal rate of fluoride ions. Considering the removal efficiency of fluoride ions, and the raw material cost of the adsorbent used, the optimum dosage of the adsorbent used is 10.0 g/dm^3 .

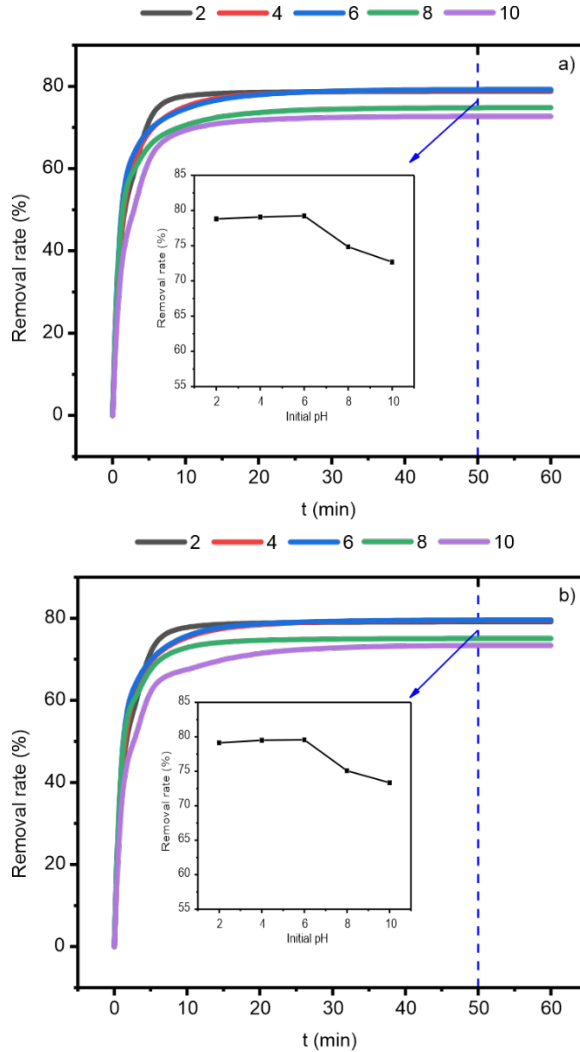


Fig. 10. Effect of initial pH on adsorption of fluoride ions for La-YK (a), and La-MJ (b) (dosage of activated carbon 10 g/dm^3 , initial F^- concentration 30.05 mg/dm^3)

Figure 10 shows the effect of the La-modified activated carbon on the removal rate of fluoride ions at $25 \text{ }^\circ\text{C}$ at different initial pH. When the initial pH increases from 2.0 to 6.0, the removal efficiency of fluoride ions increases slightly, but for pH above 6.0, the it decreases to the lowest value when pH is 10.0. It may be that when the pH is too

high, OH^- ions in the solution compete with fluoride ions for adsorption sites which will have a negative impact on the removal of fluoride ions, resulting in a rapid decrease in the removal rate. Therefore, pH should be controlled. According to the test results, the optimal initial pH value is 6.0. However, under the optimal conditions (the amount of activated carbon 10 g/dm^3 , and the initial pH 6.0), the fluoride ion concentration in the effluent is 6.14 mg/dm^3 , which cannot meet the discharge standard. Therefore, it is considered to be the secondary advanced treatment of the chemical precipitation test before, and under the joint action, it is expected to meet the discharge standard.

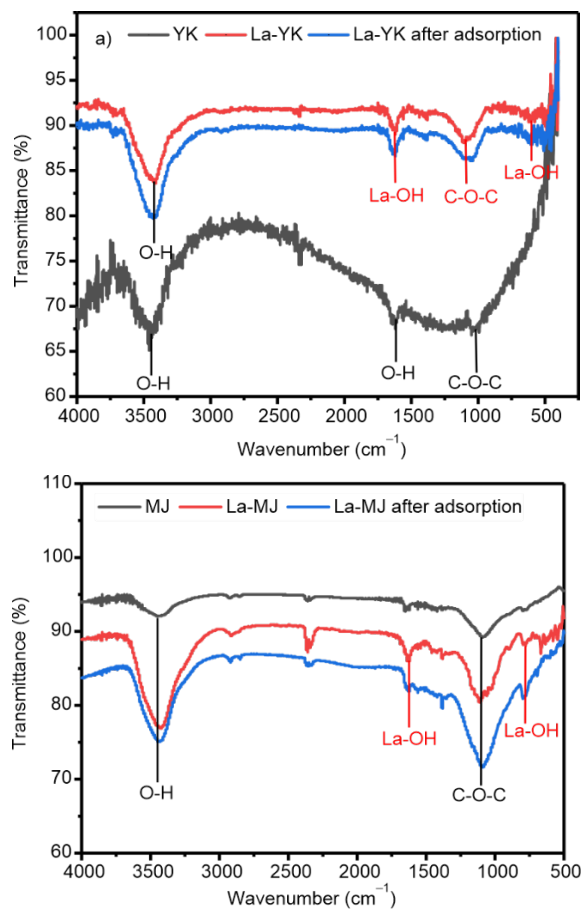


Fig. 11. Fourier transform infrared spectra of La-YK (a), and La-MJ (b)

Fourier transform infrared spectroscopy (FT-IR) was used to analyze the modified, and adsorbed activated carbon, and the results are shown in Fig. 11. $3000\text{--}3750 \text{ cm}^{-1}$ is the characteristic peak of O–H vibration; $750\text{--}1250 \text{ cm}^{-1}$ is the characteristic peak of C–O–C. In the vibration region of the two groups, the peak positions of the activated

carbon before, and after modification are similar, and there is no obvious new characteristic peak. According to the modified infrared curve, there are two characteristic peaks of La–OH at 1500–1750 cm^{-1} , and 250–500 cm^{-1} , due to the stretching and bending vibration of La–OH bond. According to the acid-base theory, because La^{3+} is Lewis acid, it is easy to complex with OH^- groups in solution and exists on the surface of activated carbon in the form of La–OH bond.

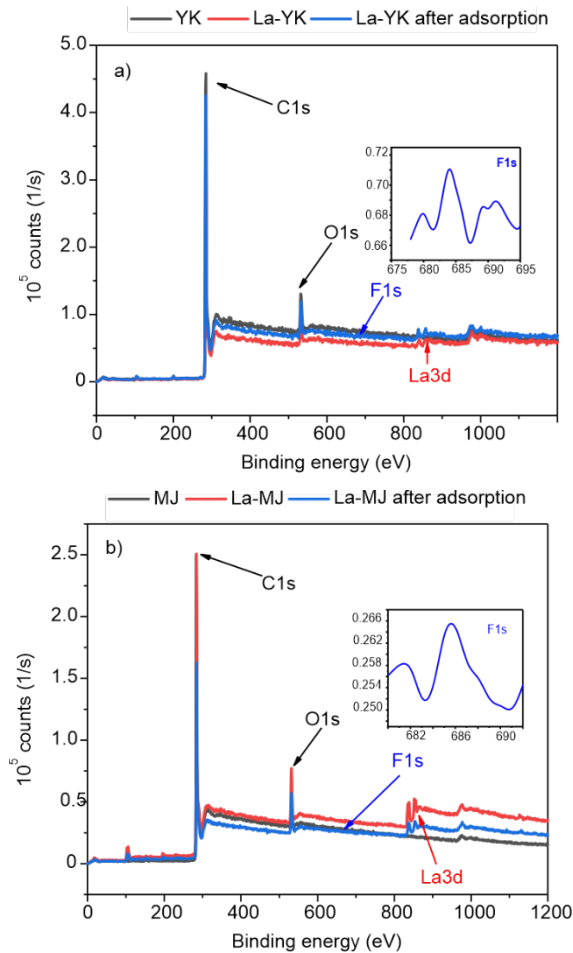


Fig. 12. X-ray photoelectron spectra (XPS) of La-YK (a), and La-MJ (b)

XPS was used to analyze the modified, and adsorbed activated carbon, and the results are shown in Fig. 12. According to Fig. 12, the binding energy of C1s electrons in activated carbon is 284 eV, and the binding energy of O1s electrons is 532 eV. The modified activated carbon does not greatly interfere with the spectral phase before modification, indicating that it does not fundamentally change its surface properties. The

modified XPS spectra showed that La3d electron appeared, and its binding energy was about 839 eV, indicating that La was successfully loaded onto the surface of activated carbon. After adsorption, F1s electrons appeared, and their binding energy was about 684 eV, indicating that fluoride ions were adsorbed onto activated carbon from the liquid phase.

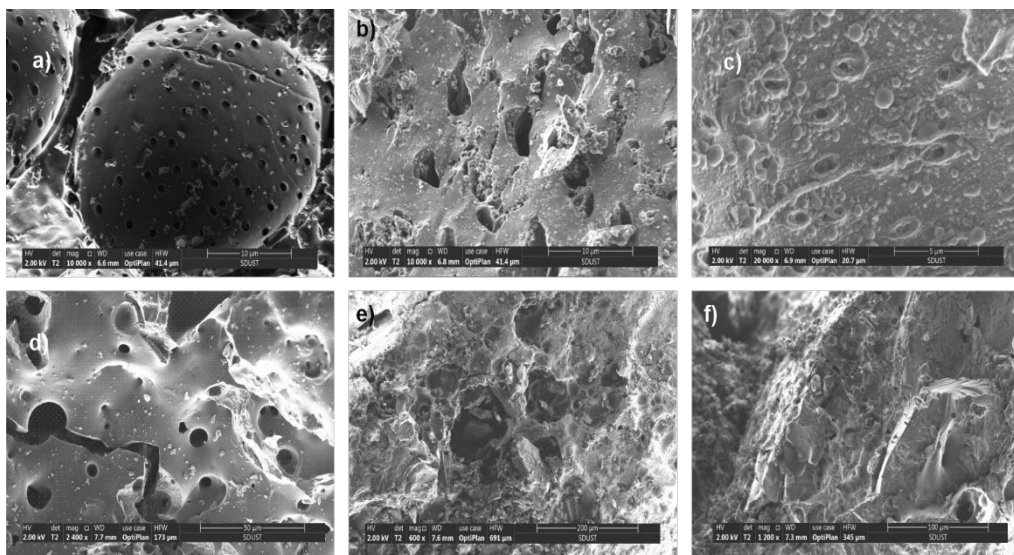


Fig. 13. SEM images of activated carbon before and after adsorption:
a) YK, b) La-YK, c) La-YK after adsorption, d) MJ, e) La-MJ, f) La-MJ after adsorption

SEM was used to observe the micro-morphology characteristics of the activated carbon surface, as shown in Fig. 13. It can be seen from Figs. 13a, d that the surface of activated carbon grains based on YK, and MJ is relatively smooth and has numerous small pores with developed pores, which also makes them have a large specific surface area, which is conducive to adsorption. In Figures 13b, c, e, and f, the scanning electron micrographs before, and after adsorption on La-YK, and La-MJ activated carbon are shown. It can be seen that some substances are attached to the pores of activated carbon through La modification. Based on the infrared spectrum analysis, it is concluded that La is loaded on the surface of activated carbon grains. Therefore, as shown in the SEM diagram after adsorption, when the activated carbon is put into the wastewater, the fluoride ions will specifically combine with La on the surface to form La-F groups, which greatly improves the removal efficiency of fluoride ions.

In order to determine the adsorption isotherm type of activated carbon, the N_2 adsorption, and desorption isotherm of La-MJ, and La-YK activated carbon were measured. The pore structure of activated carbon was determined by automatic specific surface area and porosity analyzer (BET), and the results are shown in Fig. 14.

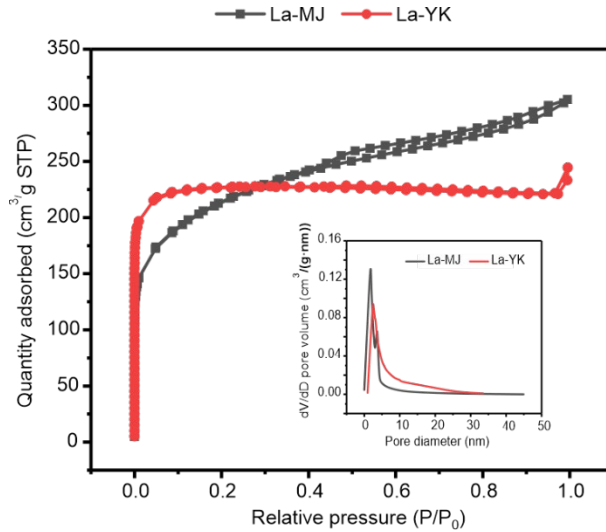


Fig. 14. Adsorption-desorption isotherms, and pore size distribution of activated carbon

Figure 14 shows the adsorption and desorption isotherms, and pore size distribution of La-MJ, and La-YK activated carbon. According to the pore size distribution diagram, the pore size distribution of activated carbon ranges mainly between 0 and 10 nm, and the pore volume of La-MJ is slightly larger than that of La-YK, which explains why the treatment effect of La-MJ is better than that of La-YK.

For La-MJ activated carbon, under the relative pressure 0–0.1, the gas adsorption capacity increases significantly, and between 0.1 and 1, the increase becomes slower. For La-YK activated carbon, under the relative pressure 0–0.1, the gas adsorption capacity increases significantly, indicating that for La-YK activated carbon adsorption occurs via internal micropores filling. When the relative pressure is 0.1–0.9, the gas adsorption capacity tends to be constant, indicating that the adsorption reaches saturation. The adsorption on La-YK belongs to the type I adsorption in the classification of the International Union of Pure, and Applied Chemistry (IUPAC), indicating that La-YK activated carbon is a microporous adsorbent that adsorbs gas through microporous filling, and the saturated adsorption value is equal to the filling volume of micropores. The adsorption isotherm of La-MJ belongs to type II adsorption isotherm; La-MJ activated carbon is a kind of mesoporous adsorbent, and the adsorption process is physical adsorption. Because of the strong interaction between the adsorbate and the surface, the adsorption increases rapidly at lower relative pressure, the curve shows a convex shape, and there is an inflection point near the single-layer adsorption. With the continuous increase of the relative pressure, the multi-layer adsorption gradually forms, and then with the increase of the adsorption layer, The adsorption capacity is also increasing.

3.4. TREATMENT OF ACTUAL FLUORINE-CONTAINING WASTEWATER BY CHEMICAL PRECIPITATION-ADSORPTION PROCESS

According to the optimal conditions, and the nature of wastewater examined, the following process flow chart was designed (Fig. 15):

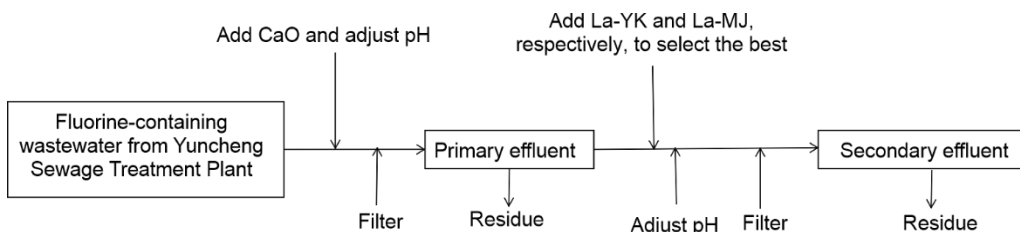


Fig. 15. Chemical precipitation-adsorption process flow chart

The properties of the primary wastewater obtained after precipitation with CaO at pH equal to 8 are shown in Table 4.

Table 4

Properties of wastewater from Yuncheng Sewage Treatment Plant after chemical precipitation

Fluoride ions concentration [mg/dm ³]	COD [(mg/dm ³)]	pH
7.76	98	9.6

A part of the fluoride ions in the wastewater precipitated with CaO, however, due to the solubility, it has not reached the discharge standard, so it needs to be further treated. The COD content is almost unchanged compared with that before treatment (Table 1), indicating that the addition of CaO has little impact on these two indicators. pH increased after the addition of CaO because a part of CaO dissolved in water, increasing the alkalinity of the solution.

Table 5

Properties of wastewater from Yuncheng Sewage Treatment Plant after La-MJ, and La-YK treatment

Additive	Fluoride ions concentration [mg/dm ³]	COD [mg/dm ³]	pH
La-MJ	1.26	47	6.5
La-YK	1.45	52	6.7

The characteristics of the secondary effluent, obtained after adsorption with La-YK or La-MJ activated carbon at pH equal to 6.0 is shown in Table 5. After treatment, the

fluorine-containing wastewater can meet the discharge standard. The concentration of fluoride ions after La-MJ treatment reached 1.26 mg/dm^3 , which is better than La-YK (1.45 mg/dm^3). The fluoride ion removal rate of the final effluent is as follows: La-MJ 95.81%, La-YK is 95.17%.

4. CONCLUSIONS

- The test of coagulation, and sedimentation conditions of poly aluminum sulfate showed that the optimum dosage of poly aluminum sulfate was 0.3 g/dm^3 , and the optimum initial pH value of coagulation, and sedimentation test was 4.0. The removal rate of fluoride ions reached 98.46%, and their concentration in fluorine-containing wastewater was 0.462 mg/dm^3 , which reached the discharge standard (1.5 mg/dm^3). According to XPS analysis, the removal of fluorine ions by poly aluminum sulfate also took place through a chemical reaction in addition to electrostatic adsorption, and the contents of Al^{3+} ions was reduced in the reaction process.

- For CaO chemical precipitation-activated carbon loaded with lanthanum, the optimum dosage of CaO was 20 g/dm^3 , and the optimum initial pH was 8.0. The optimum amount of activated carbon loaded with lanthanum was 10 g/dm^3 , the optimum initial pH was 6.0, and the treatment effect of La-MJ was better than that of La-YK. The removal rate of fluoride ions reached 95.81%, and their concentration in fluorine-containing wastewater was 1.26 mg/dm^3 , which met the discharge standard. The pore volume of La-MJ was slightly larger than that of La-YK, which explains why the treatment effect of La-MJ was better than that of La-YK.

- The poly aluminum sulfate coagulation-sedimentation method is more suitable for the treatment of fluorine-containing wastewater from Yuncheng Sewage Treatment Plant, regardless of the treatment cost or the ease of operation. The secondary treatment method by CaO chemical precipitation-activated carbon adsorption loaded with lanthanum can be used to treat fluorine-containing wastewater with high concentrations.

ACKNOWLEDGEMENTS

The authors acknowledge the Research Institute for Mineral Processing, Shandong University of Science and Technology for funding this work.

REFERENCES

- [1] BERA B., BHATTACHARJEE S., CHAMLING M., GHOSH A., SENGUPTA N., *Fluoride hazard, and risk enumeration of hard rock unconfined aquifers in the extended part of Chhota Nagpur Gneissic Complex*, J. Geol. Soc. India, 2021, 97, 199–209. DOI: 10.1007/S12594-021-1651-0.
- [2] THANGAVELU A., SAPNA K., PRABITHA R., *Assessment of fluoride hazard in groundwater of Palghat District, Kerala. A GIS approach*, Int. J. Environ. Pollut., 2019, 66 (1–3), 187–210.

- [3] DAVIS L., HANIA R., BOOMSTRA D., ROSSOUW D., CHARPIN J.F., UHLIR J., MARACEK M., *Radiolytic production of fluorine gas from MSR relevant fluoride salts*, Nucl. Sci. Eng., 2023, 197 (4), 633–646. DOI: 10.1080/00295639.2022.2129951.
- [4] TOYODA A., TAIRA T., *A new method for treating fluorine wastewater to reduce sludge, and running costs*, IEEE Trans. Semicond. Manuf., 2000, 13 (3), 305–309. DOI: 10.1109/66.857940.
- [5] KIM D., YOON M., CHUN Y.T., LEE J., *Effect of fluorine–fluorine repulsive coupling on charge transport in cyclopentadithiophene-based donor–acceptor-type conjugated copolymer films*, Org. Electron., 2022, 101, 106402. DOI: 10.1016/J.ORGEL.2021.106402.
- [6] MA Y., DING A., DONG X., ZHENG S., WANG T., TIAN R., HUANG H., *Low-temperature resistance of fluorine rubber with modified Si-based nanoparticles*, Mater. Today Commun., 2022, 33, 104947. DOI: 10.1016/J.MTCOMM.2022.104947.
- [7] TAN M., LI T., WANG Z., SHANG B., DANG J., *Investigation on adsorption of sodium fluoro-aluminates on graphite by density functional theory*, J. Mol. Liq., 2023, 373, 121252. DOI: 10.1016/J.MOLLIQ.2023.121252.
- [8] KOLOBKOVA E., *Fluoroaluminate glasses with low phosphate content doped with Er³⁺/Yb³⁺ ions for up-conversion luminescence temperature sensors*, Mater. Chem. Phys., 2022, 290, 126575. DOI: 10.1016/J.MATCHEMPHYS.2022.126575.
- [9] RUDSKOI A.I., PARSHIN S.G., RUDSKOI A.I., PARSHIN S.G., *Electrochemical removal of hydroxyl, and diffusible hydrogen in aluminum fluoride slags of welding flux-cored wires*, Dokl. Chem., 2022, 504 (2), 118–121. DOI: 10.1134/S0012500822700033.
- [10] IRMALENY I., HIDAYAT O.T., YOLANDA Y., TOBING E.L., *Comparative evaluation of the increase in enamel hardness post-external bleaching after using casein phosphopeptide amorphous calcium phosphate fluoride (CPP-ACPF), and 5% sodium fluoride (NaF) remineralizing agents*, Eur. J. Dent., 2023, Jan. 30. DOI: 10.1055/S-0043-1761189.
- [11] NAIR M., PATIL R., BAHUTULE S., *Comparative evaluation of hydroxyapatite fluoride, and casein phosphopeptide amorphous calcium phosphate fluoride as remineralizing agents in primary teeth using pH cycling, and single-sectioning technique*, Int. J. Med. Oral Res., 2022, 7 (2), 31–35. DOI: 10.4103/IJMO.IJMO_15_22.
- [12] DESAI S., RAO D., PANWAR S., KOTHARI N., GUPTA S., *An in vitro comparative evaluation of casein phosphopeptide-amorphous calcium phosphate fluoride, tricalcium phosphate, and grape seed extract on remineralization of artificial caries lesion in primary enamel*, J. Clin. Pediatr. Dent., 2022, 46 (5), 72–80. DOI: 10.22514/JOCPPD.2022.010.
- [13] MEKKY A.I., DOWIDAR K.M.L., TALAAT D.M., *Casein phosphopeptide amorphous calcium phosphate fluoride varnish in remineralization of early carious lesions in primary dentition. Randomized clinical trial*, Pediatr. Dent., 2021, 43 (1), 17–23.
- [14] SURYANI H., GEHLOT P., MANJUNATH M., *Evaluation of the remineralisation potential of bioactive glass, nanohydroxyapatite, and casein phosphopeptide-amorphous calcium phosphate fluoride-based toothpastes on enamel erosion lesion. An ex vivo study*, Indian J. Dent. Res., 2020, 31 (5), 670–677. DOI: 10.4103/ijdr.IJDR_735_17.
- [15] HANJOO J., KYUNG H.K., MIN-JUNG J., YOUNG-SEAK L., *Fluorination effect of activated carbons on performance of asymmetric capacitive deionization*, Appl. Surf. Sci., 2017, 409, 117–123. DOI: 10.1016/j.apsusc.2017.02.234.
- [16] KIM M.J., JUNG M.J., CHOI S.S., LEE Y.S., *Effects of the fluorination of activated carbons on the chromium ion adsorption*, Appl. Chem. Eng., 2015, 26 (1), 92098. DOI: 10.14478/ACE.2014.1126.
- [17] SEMASHKO V.V., KORABLEVA S.L., FEDOROV P.P., *Lithium rare-earth fluorides as photonic materials. 2. Some physical, spectroscopic, and lasing characteristics*, Inorg. Mater., 2022, 58 (5), 447–492. DOI: 10.1134/S0020168522050028.

- [18] FEDOROV P.P., SEMASHKO V.V., KORABLEVA S.L., *Lithium rare-earth fluorides as photonic materials: 1. Physicochemical characterization*, Inorg. Mater., 2022, 58 (3), 223–245. DOI: 10.1134/S0020168522030049.
- [19] YANG S., ERKO A., RIMAN R.E., NAVROTSKY A., *Thermochemistry of stoichiometric rare earth oxyfluorides REOF*, J. Am. Ceram. Soc., 2022, 105 (7), 1472–1480. DOI: 10.1111/JACE.18429.